
**TRIPLE-CRYSTAL X-RAY DIFFRACTOMETRY STUDY
OF THE DECOMPOSITION KINETICS IN A SOLID
SOLUTION OF OXYGEN IN Cz-SILICON****M.M. NOVIKOV**, P.O. TESELKO, O.V. MYKHALYUKPACS 61.10.-i;61.72.Dd;61.72.Lk; Taras Shevchenko National University of Kyiv, Faculty of Physics
61.72.Tt;61.72.Yx;07.85.Jy (2, Academician Glushkov Ave., Bld. 1, Kyiv 03680, Ukraine; e-mail: peter@univ.kiev.ua)©2009

The method of triple-crystal X-ray diffractometry is used to study the process of formation and growth of defects (precipitates and dislocation loops) at the isothermal decomposition of a supersaturated solid solution of oxygen in Cz-grown silicon. A technique for the experimental determination of defect distributions by size and concentration is proposed and tested. The sections of distribution curves are obtained, which correspond to the capabilities of X-ray detection of local defects. The growth of oxygen-containing precipitates is found to take place due to the diffusion processes, whereas the formation of dislocation loops is due to the processes of coagulation of silicon interstitial atoms and the extrusion of loops by stresses around the precipitates.

1. Introduction

The overwhelming fraction of silicon used in the electronic industry was grown by the Czochralski method (Cz-Si). The main background impurity in it is oxygen, the concentration of which reaches $10^{17} \div 10^{18} \text{ cm}^{-3}$. Therefore, oxygen in Cz-Si governs not only a number of electrophysical properties of a crystal, but also the structural characteristics of silicon. During technological heat treatments, when the mobility of oxygen atoms grows and their solubility falls down, oxygen forms oxygen-containing complexes (precipitates) of various kinds, the growth of which is related to a decrease of the free energy of the crystal. The processes of emergence and growth of oxygen-containing complexes were studied in a number of works, among which the works devoted to direct electron microscopy observations should be distinguished [1–4]. The authors of those works found that the configuration of defects depends on the prehistory of studied crystals. The generation and the growth of defects belonging to that or another type

are affected, first of all, by the previous heat treatment of specimens [4]. Such an assumption was theoretically substantiated, when the temperature dependence of the precipitate critical radius was analyzed [5, 6]. Complexes nucleated at a certain temperature continue to grow at the subsequent annealing, provided that their radii exceed the critical one under given conditions [5]. However, a shortcoming of electronic microscopy is the circumstance that it makes difficult to gather a large body of statistical data. To solve this problem, selective chemical etching [5] and infra-red spectrometry [7] are used. After a series of theoretical works devoted to dynamic X-ray scattering [8–11] have been published, X-ray diffractometry is also used to overcome those difficulties [12–14].

To date, the most sensitive methods for the registration of scattered X-ray radiation are double- and triple-crystal X-ray diffractometries. The latter is more informative, because it allows the diffusion and coherent fractions of scattered rays to be distinguished experimentally. The application of a dynamic theory enables both the diffraction and physical characteristics of scattering centers, such as their dimensions and concentration, to be determined. The centers of X-ray radiation scattering are local defects (the clusters of intrinsic defects and precipitates formed from impurity atoms) and dislocation loops. The deformation-associated fields of stresses around those centers are responsible for the diffuse scattering at X-ray diffraction by perfect enough crystals. Already the first attempts to determine the average dimensions and the concentration of defects, which arise in the course of annealing of silicon single crystals after the implantation of silicon ions [15] or during

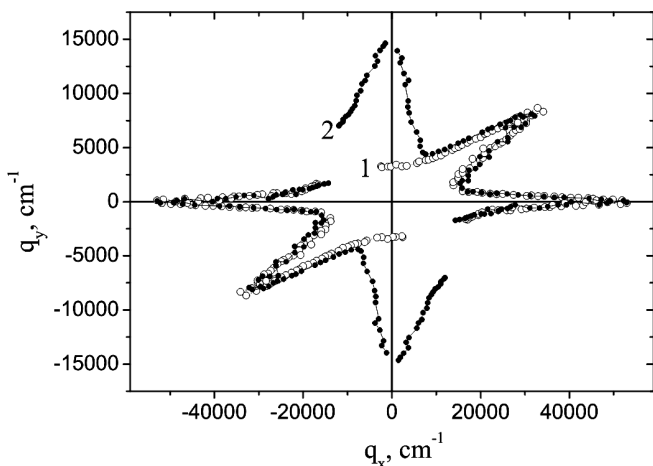


Fig. 1. Maps of intensity distribution (44 pulse/s) near site (111) of the reciprocal lattice for specimens annealed at 900 °C for 6 (1) and 50 h (2)

the decomposition of a solid solution of oxygen [11, 16], demonstrated the high efficiency and the rapidity of this method. The accuracy of diffractometry researches was checked by making a comparison of their results with the data of electron microscopy researches. In later works, the technique for the determination of a type of scattering centers – precipitates or dislocation loops – was proposed [12, 17]. It should be noted that, in the course of dissolution and coagulation of decomposition particles, there must exist the spectra of their distributions over the dimension and the concentration, which are observed in electron microscopy researches [4, 15]. It is evident that those distributions must reveal themselves in the data of diffractometry researches. Therefore, one of the purposes of this work was to determine whether the detection and the quantitative determination of the distribution with the help of triple-crystal X-ray diffractometry are possible.

In addition, our another purpose was the application of the methods of triple-crystal X-ray diffractometry to the study of the kinetics of variations of dimensions and concentrations of defects that are being formed. It is especially interesting, because we practically know nothing about similar works. Based on the data presented in work [4], we selected the annealing temperature for a specimen to be 900 °C. At this temperature, the initial annealing of crystals gives rise to the formation of the simplest spectrum of defects; namely, these are lamellar SiO_x precipitates and perfect dislocation loops. The measurement and calculation techniques were considered in work [14], with small variations being described below.

2. Methodological Features and Experimental Data

Specimens for researches were cut out from a factory-fabricated polished Cz-Si plate KEF-2.0 with the surface orientation (111) and were subjected to the additional chemical polishing. Data were registered by the 2θ scanning method at the Bragg symmetric reflection of $\text{Cu}_{K\alpha 1}$ radiation. The incident beam intensity was about 10^5 pulse/s. The specimens were annealed in air, and the oxide layer that had formed on the surface was removed in fluoric acid.

In the diffraction patterns obtained for specimens with a short annealing time, only the lateral and main maxima were observed. The sensitivity threshold of a diffractometer did not allow us to measure the small contribution given by diffuse scattering by a monochromator to the measured diffuse scattering. Therefore, we did not consider this contribution. As the annealing time increased, the intensity of diffuse scattering grew, and the diffraction patterns obtained for specimens that had been annealed for more than 15 h had an ordinary three-peak form (Fig. 1). In the interval of average and large angles of a deviation of the specimen from the Bragg position ($\alpha \geq 20''$), the peaks can be resolved well. As α increased further, the intensity of peaks decreased. In this work, only the results obtained at positive deviation angles of the specimen are presented. Reference measurements at negative deviation angles revealed no antisymmetry in the diffuse scattering. Since the time required for studying even one specimen was long enough, the complete research at negative deviation angles was not carried out.

The preliminary computer-assisted data processing allowed the peak and integral intensities of diffraction maxima to be determined for any α [14]. The vector magnitude $k_m = 2\pi/R_0$ describes the boundary between the Huang and Stokes–Wilson regions in the diffuse scattering distribution. In work [18], this boundary was analyzed for silicon specimens. On the basis of the results obtained in work [18] and the data of electron microscopy researches [4], we did not take the contribution of scattering in the Stokes–Wilson region into account.

It is known [9, 10, 12] that the integral intensity of the diffusion maximum is described by the relation

$$R_{\Sigma}(\alpha) = \frac{I_{D\Sigma}}{I_0} = \frac{cC^2E^2m_0j(k_0)}{2\mu_0} \quad (1)$$

at small (less than 1 μm) scattering center dimensions. Similarly, for the main peak,

$$R_M = \frac{I_M}{I_0} = \frac{C^2 |\chi_{\text{Hr}}|^2 E^2}{4 \sin^2 2\theta_B \alpha^2}, \quad (2)$$

where C is the polarization factor, $E = \exp(-L)$ is the Debye–Waller static factor, $m_0 = 0.169 \text{ cm}$ is the constant of (111) reflection from silicon, $|\chi_{\text{Hr}}|$ is the absolute value of the Fourier component of the crystal polarization, μ_0 is the absorption factor, and θ_B is the Bragg angle. The function $j(k_0) = B(AR_0^2\alpha^2 - \ln R_0\alpha - b)$, where, if the scattering centers are clusters, $B = B_K$, $A = 2.081 \times 10^{14} \text{ cm}^{-2}$, and $b = 17.183$, and, if the scattering occurs at dislocation loops, $B = B_D = 4.1036 \times 10^{30} R_0^4$, $A = 4.252 \times 10^{13} \text{ cm}^{-2}$, and $b = 16.835$. On the basis of data obtained in work [4], we assume that precipitates have mainly lamellar shape at the early annealing stage and, in the course of growing, become spheroidal. By using the geometric mean of their volume $V_P = \sqrt{V_c V_n}$, where $V_c = \frac{4}{3}\pi R_P^3$ and $V_n = \pi R_P^2 h_P$ at $h_P \approx 6.08 \times 10^{-5} R_P^{0.4}$ [14], we obtain $B_K = 2.32 \times 10^{39} R_P^{5.4}$ for the reflection concerned, and the precipitate volume $V_P = 9 \times 10^{-3} R_P^{2.7}$. Note that, in all formula given above, R is expressed in terms of centimeter units and α in terms of radians.

Then, the ratio of the intensities of the diffusion peak and the main one is

$$Q = \frac{R_\Sigma(\alpha)}{R_M} = \frac{2cm_0 \sin^2 2\theta_B j(k_0)\alpha^2}{\mu_0 |\chi_{\text{Hr}}|^2}. \quad (3)$$

The last formula does not depend on the incident beam intensity I_0 and the errors of the specimen arrangement on a goniometer [13]. The extrapolation of the ratio Q/α^2 to the zero α -value following the technique described in work [14] makes it possible to evaluate the dimensions of clusters, R_P , and dislocation loops, R_D , whereas the slopes of the corresponding straight lines $\frac{d(Q/\alpha^2)}{d \ln \alpha}$ allow us to find the concentrations c_P and c_D of those defects.

The presence of two straight sections with different slopes, which are observed in the plots for the quantity $Q/\alpha^2 - \ln \alpha$ (Fig. 2), is interpreted as a result of the scattering by dislocation loops (the straight line with a large slope) and by precipitates. However, both sections in the plot are not perfectly straight lines. It can be explained by the distributions of scattering centers of both types over their dimensions and concentrations.

Substituting relevant numerical data into expression (3) and taking into account that the scattering occurs

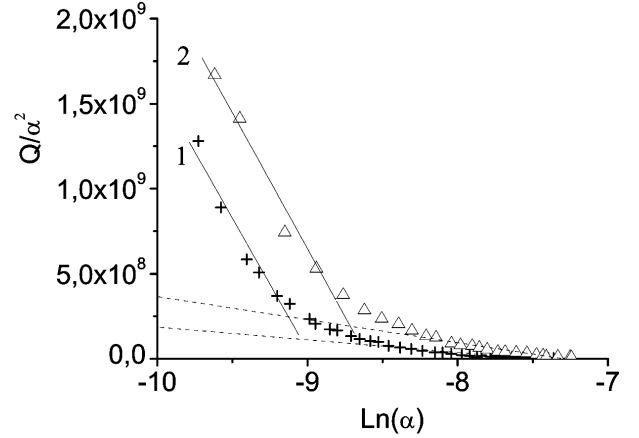


Fig. 2. Dependences of the quantity Q/α^2 on the logarithm of the deviation angle for specimens annealed for 50 (1) and 70 h (2)

at both precipitates and dislocation loops with various dimensions and corresponding concentrations, we obtain

$$\begin{aligned} \frac{Q}{\alpha^2} = & 2.95 \times 10^{37} \sum_i c_{di} R_{di}^4 \left[4.252 \times 10^{13} R_{di}^2 \alpha^2 - \right. \\ & \left. - \ln(R_{di}\alpha) - 16.835 \right] + 1.98 \times 10^{46} \sum_k R_{pk}^{5.4} c_{pk} \times \\ & \times \left[2.081 \times 10^{14} R_{pk}^2 \alpha^2 - \ln(R_{pk}\alpha) - 17.183 \right]. \quad (4) \end{aligned}$$

In this formula, every term on its right hand side vanishes at certain R - and C -values due to the zeroing of the corresponding expression in brackets. It enables a straight line that passes through every pair of experimental points to be extrapolated to zero separately. As a result, we obtain a set of experimental results, which correspond to the right (cluster) sections of the curves, because the value of $j(k_0)$ for dislocation loops with dimensions of about 10^{-4} cm and at $\ln \alpha$ of about -8.5 is practically equal to zero. Grouping the data obtained within the intervals of R -variation gives an opportunity to plot the histogram for the distribution of experimentally revealed precipitates over their dimensions (Fig. 3). The accuracy of histograms depends drastically on the number of experimental points. In our case, the accuracy was about 20%. The histogram transforms into the distribution curve only if the number of points is of the order of $100 \div 150$. It is very difficult to obtain such a number of diffraction patterns at various α , which is associated with rather a low intensity of the primary X-ray beam, so that large rotation angles of a specimen cannot be used.

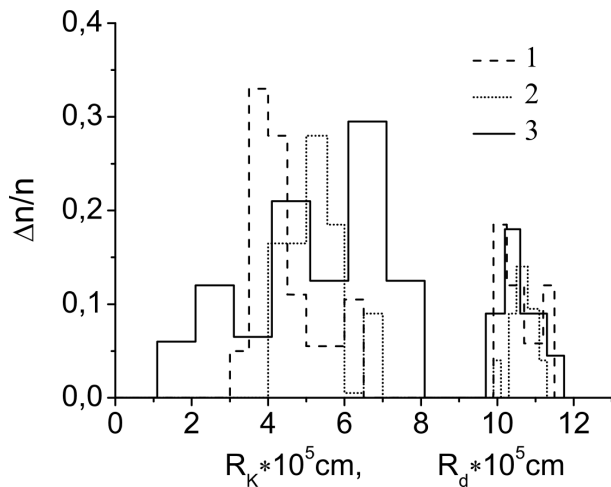


Fig. 3. Histograms of the distribution of experimentally revealed precipitates (the left group) and dislocation loops (the right group) over their radii. Annealing time is 30 (1), 50 (2), and 70 h (3)

The substitution of obtained R -values with regard for their relative number into Eq. (4) allows the concentration of precipitates with that or another radius to be calculated, as well as the total concentration of local defects revealed by the X-ray diffraction method. The obtained distribution of the concentrations of precipitates over their dimensions is presented in Fig. 4 (the left group).

Making use of Eq. (4), the curve for the quantity Q/α^2 , which corresponds to the radiation scattering by clusters, can be prolonged to the range of small α (dashed lines in Fig. 2) and subtracted from the experimental curve obtained for this region. The remainder corresponds to the dislocation scattering. Therefore, carrying out a calculation procedure that is similar to the described one, it is possible to find the distributions of dislocation loops over dimensions and concentrations. These data are presented in Figs. 3 and 4.

3. Discussion of the Data Obtained

Our calculations of the average dimensions and the total concentrations of defects (see the results in the table) showed their quite good agreement with most probable values.

It is clear that the growth of the dimension of precipitates in the course of annealing is governed by the diffusion of oxygen atoms to an oxygen-containing center. Over the time interval t , oxygen atoms located in the volume $V = 4/3\pi r^3$, where $r \approx \sqrt{2Dt}$ and D is the diffusion coefficient, gather at its center. Provided

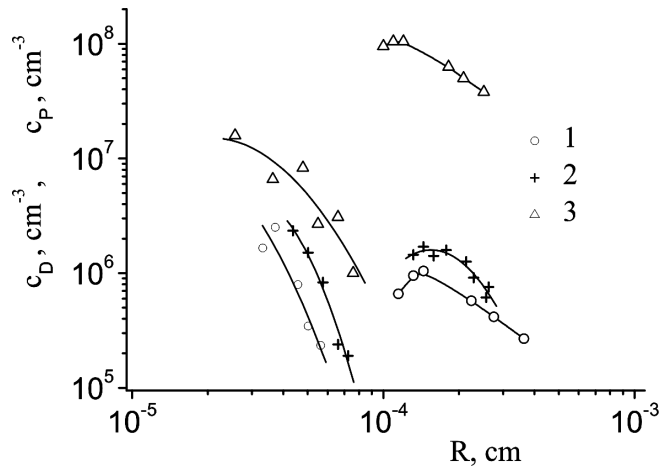


Fig. 4. Dependences of the defect concentration on their dimensions: precipitates (the left group) and dislocation loops (the right group). Annealing time is 30 (1), 50 (2), and 70 h (3)

that a unit volume of silicon contains Δn_0 extra oxygen atoms—with respect to the solubility threshold at a given temperature,— $V\Delta n_0$ of them get into the precipitate, so that the volume of the latter becomes equal to $V_D = V\Delta n_0 V_0$, where V_0 is the volume occupied by one oxygen atom. Hence, $V\Delta n_0 V_0 = \sqrt{V_c V_n} = 9 \times 10^{-3} \pi R_P^2$. Whence we obtain

$$R_P^{2.7} = 4.19 \times 10^2 \Delta n_0 V_0 (Dt)^{3/2}. \tag{5}$$

In Fig. 5, the experimental dependence of $\ln R_p$ on $\ln t$ is depicted. It is described well enough by a straight line with a slope of about 0.6, which corresponds to formula (5). Taking $\Delta n_0 \approx 5 \times 10^{17} \text{ cm}^{-3}$ [19] and assuming the volume per one oxygen atom in the coesite structure to be approximately 50 Å, we obtain $D \approx 2 \times 10^{-12} \text{ cm}^2/\text{s}$, which correlates rather well with the known literature data on the diffusion coefficient of oxygen in this temperature range ($3 \times 10^{-12} \text{ cm}^2/\text{s}$ [20]).

The application of the approach described above to the data of work [14] on the temperature dependence of precipitate dimensions, provided that the annealing time is fixed, enables the activation energy of oxygen diffusion in silicon to be evaluated. Really, if $D = D_0 \exp\left(-\frac{Q}{kT}\right)$,

Variations of average dimensions and concentrations of precipitates and dislocation loops in the course of annealing

$t, \text{ h}$	$R_P \times 10^5, \text{ cm}$	$c_P \times 10^{-7}, \text{ cm}^{-3}$	$R_D \times 10^4, \text{ cm}$	$c_D \times 10^{-8}, \text{ cm}^{-3}$
15	2.81	9.7	2.05	0.96
30	3.78	2.4	2.36	0.78
50	4.85	1.28	2.90	2.25
70	6.01	2.18	3.24	2.63

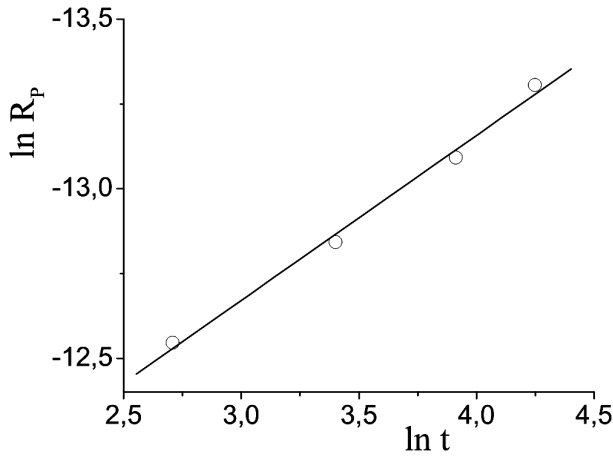


Fig. 5. Dependence of the precipitate radius logarithm on the annealing time logarithm

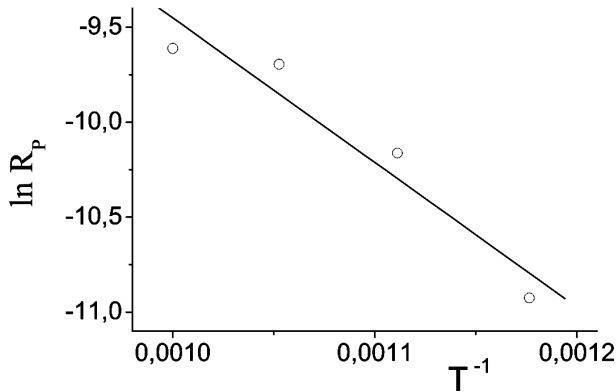


Fig. 6. Dependence of $\ln R_p$ on $1/T$

then the dependence of $\ln R_p$ on $1/T$ must be linear, according to formula (5), and its slope can be used to determine Q . According to the data exhibited in Fig. 6, $Q = 2.17$ eV, whereas the literature value for this quantity is 2.44 eV [20].

The formation of oxygen-containing precipitates gives rise to the appearance of elastic stresses in the silicon matrix owing to the difference between the molecular volumes of oxide and silicon. Therefore, the Debye–Waller static factor has to change in the course of annealing. According to Eq. (2), $\Delta \ln R_M = 2\Delta L$ if $\alpha = \text{const}$. On this basis, we used the experimental data depicted in Fig. 7 to calculate ΔL . It turns out that the increment of this quantity with increase in the annealing time is insignificant and is at most 0.1. The latter circumstance can be explained by the relaxation of elastic stresses owing to the emission of silicon interstitial atoms from the precipitate into the matrix (approximately 0.5 silicon atoms per one oxygen atom attached to the pre-

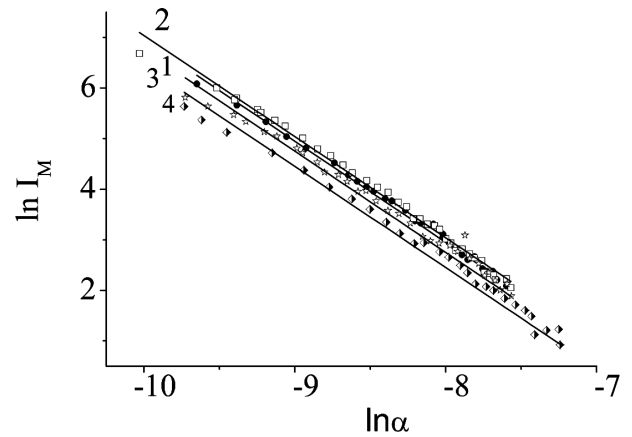


Fig. 7. Dependences of the logarithm of the main peak intensity on the rotation angle logarithm for specimens annealed for 3 (1), 15 (2), 50 (3), and 70 h (4)

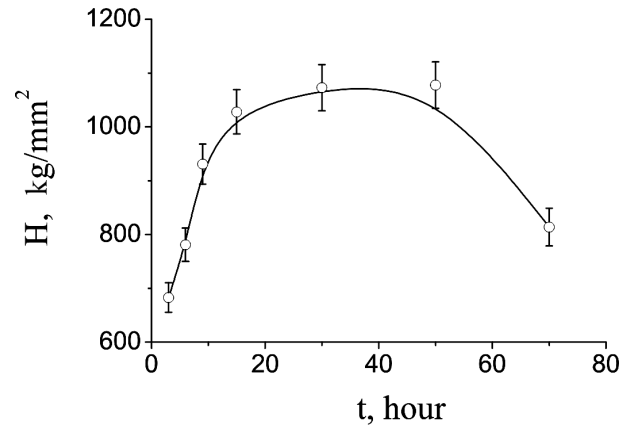


Fig. 8. Dependence of the silicon microhardness on the annealing time

cipitate [4]). Later on, the penetrated silicon atoms form perfect dislocation loops and package defects in the matrix. By comparing the corresponding volumes, it is easy to evaluate the concentration of dislocation loops formed in such a process. It turns out to be approximately four times lower than that quoted in the table. This discrepancy takes place, in our opinion, due to the extrusion of dislocation loops by the stress field around the precipitates which occurs in parallel to the considered process. Such a mechanism of the formation of loops was observed in electron microscopy studies [2, 4], and it may probably be responsible for the growth of the loop concentration in the course of annealing.

The formation of dislocation loops has to invoke the variation of mechanical characteristics of the crystal. We observed the growth of microhardness in the course of annealing (Fig. 8). However, as the dimensions of defects increase, the microhardness growth curve saturates.

Such a variation of the microhardness, which accompanies the decomposition of a solid solution, is characteristic of many substances. In particular, it is observed during the ageing of aluminum alloys.

4. Conclusions

Using the method of triple-crystal X-ray diffractometry, the kinetics of the decomposition of an oxygen solid solution in Cz–Si followed by the coagulation of decomposition products into oxygen-containing precipitates and the formation of dislocation loops has been studied.

The technique proposed in this work for the data processing allows one to determine the average dimensions and the concentrations of defects, which were formed due to the coagulation of decomposition products emerging in the course of decay of solid solution of oxygen in silicon, and to obtain the defect distributions over dimensions and concentrations. These distributions led us to some interesting conclusions. The smaller the cluster dimensions, the higher is their concentration. However, we did not succeed to obtain the concentration distribution maximum by the X-ray diffraction method. This circumstance is obviously associated with the fact that the defect dimensions turned out smaller than 10^{-6} cm, whereas the diffuse scattering intensity depends drastically enough ($\propto R^4 \div R^5$) on the dimensions of scattering centers. At annealing temperatures below 1000 °C, the average dimension of defects is less than 1 μm , and the low-dimensional section of the distribution does not reveal itself. Probably, that is why long-term annealing treatments at temperatures of 1000 \div 1100 °C were used in the majority of works on X-ray researches of the precipitation processes in silicon [11, 17]. The sizes of dislocation loops are a little larger than those of precipitates; therefore, the curves of the dependence of the dislocation loop concentration on the loop radius reveal a pronounced maximum.

It is important to note that, with increase in the annealing time, the curves of the cluster distribution over the concentration shift into the region of larger dimensions. As a result, the observable concentration of clusters grows with the annealing time. It can only mean a reduction of the number of small precipitates, because their total number is determined by initial conditions, mainly, by the annealing temperature [5]. As to dislocation loops, their most probable dimensions depend weakly on the annealing time, and their concentration grows in this case. This means, in our opinion, that the formation of dislocation loops at the decomposition of the oxygen solid solution is related to both the coagu-

lation of imbedded silicon atoms and the extrusion of loops due to stresses in the vicinity of oxygen-containing precipitates; the latter grow with the coagulants.

Thus, we have established that the growth of oxygen-containing precipitates occurs due to diffusion processes, which is evidenced by the coincidence of the calculated diffusion coefficient and the activation energy of oxygen diffusion in silicon with the corresponding literature data. The formation of dislocation loops is associated with both the process of coagulation of imbedded silicon atoms and the stresses around oxygen-containing precipitates.

At the early stages of annealing, the formation of defects changes the mechanical characteristics of Czochralski-grown silicon. In particular, the growth of microhardness by approximately 20% was observed. With increase in the annealing time, the microhardness saturates.

1. M. Reiche, J. Reichel, and W. Nitzche, *Phys. Status Solidi A* **107**, 851 (1988).
2. H. Bender and J. Vanhollemont, *Phys. Status Solidi A* **107**, 455 (1988).
3. W. Bergholz and W. Schroter, in *Proc. of the 7-th International School "Defects in Crystals" (Szczyrk, Poland)*, edited by E. Mizera (World Scientific, Singapore, 1985), p. 196.
4. H. Bender, *Phys. Status Solidi A* **86**, 245 (1984).
5. K.F. Kelton, R. Falster, D. Gambaro, M. Olmo, M. Comara, and P.F. Wei, *J. Appl. Phys.* **85**, 8097 (1999).
6. J. Vanhellemont and C. Claeys, *J. Appl. Phys.* **62**, 3960 (1987).
7. M. Stavola, *Physica B* **146**, 199 (2002).
8. M.A. Krivoglaz, *Diffusion Scattering of X-Rays and Neutrons by Fluctuations* (Springer, Berlin, 1996).
9. E.N. Gavrilova, E.N. Kislovskii, V.B. Molodkin, and S.I. Olikhovskii, *Metallofizika* **14**, 70 (1992).
10. V.G. Bar'yakhtar, E.N. Gavrilova, V.B. Molodkin, and S.I. Olikhovskii, *Metallofizika* **14**, 68 (1992).
11. V.V. Nemoshkalenko, V.B. Molodkin, S.I. Olikhovskii, E.N. Kislovskii *et al.*, *Metallofizika* **15**, 53 (1993).
12. S.I. Olikhovskii, V.B. Molodkin, E.N. Kislovskii, E.G. Len, and E.V. Pervak, *Phys. Status Solidi B* **231**, 213 (2002).
13. V.B. Molodkin, V.V. Nemoshkalenko, S.I. Olikhovskii, E.N. Kislovskii, O.V. Reshetnyk, T.P. Vladimirova, V.P. Krivitsky, V.F. Machulin, I.V. Prokopenko, G.E. Ice, and B.C. Larson, *Metallofizika* **20**, 29 (1998).
14. V.A. Makara, N.N. Novikov, and V.D. Patsai, *Fiz. Tverd. Tela* **47**, 1791 (2005).

15. P. Zaumseil, U. Winter, F. Cembali, M. Servidori, and Z. Sourek, *Phys. Status Solidi A* **100**, 95 (1987).
16. V.V. Nemoshkalenko, V.B. Molodkin, S.I. Olikhovskii, E.N. Kislovskii *et al.*, *Metallofizika* **15**, 53 (1993).
17. E.M. Kislovskii, S.I. Olikhovskii, V.B. Molodkin, E.G. Len, T.P. Vladimirova, *Metallofizika* **22**, 21 (2000).
18. M.M. Novikov and B.D. Patsai, *Ukr. Fiz. Zh.* **50**, 93 (2005).
19. V.M. Babich, N.I. Bletskan, and E.F. Venger, *Oxygen in Silicon Single Crystals* (Interpress, Kyiv, 1997) (in Russian).
20. J.C. Mikkelsen, *Appl. Phys. Lett.* **40**, 336 (1982).

ВИКОРИСТАННЯ МОЖЛИВОСТЕЙ ТРИКРИСТАЛЬНОЇ
X-ДИФРАКТОМЕТРІЇ ДЛЯ ВИВЧЕННЯ КІНЕТИКИ
РОЗПАДУ ТВЕРДОГО РОЗЧИНУ
КИСНЮ В Cz-КРЕМНІЇ

М.М. Новиков, П.О. Теселько, О.В. Михалюк

Резюме

У роботі методом трикристальної рентгенівської дифрактометрії виконано дослідження процесу утворення та росту дефектів (преципітатів і дислокаційних петель) під час ізотермічного розпаду пересиченого твердого розчину кисню у Cz-кремнії. Згідно з запропонованою методикою виконано спробу експериментального визначення розподілу дефектів за розмірами і концентраціями. Отримано ділянки кривих розподілу, що відповідають можливостям рентгенівського виявлення локальних дефектів. Встановлено, що зростання кисневмісних преципітатів відбувається за рахунок протікання дифузних процесів, а утворення дислокаційних петель зв'язано як із процесами коагуляції занурених атомів кремнію, так і з видавлюванням петель напругами, що створюються навколо преципітатів.

Received 01.10.07.

Translated from Ukrainian by O.I. Voitenko